Article

Crystal Structure and Diffusion Path in the Fast Lithium-Ion Conductor La$_{0.62}$Li$_{0.16}$TiO$_3$

Masatomo Yashima, Mitsuru Itoh, Yoshiyuki Inaguma, and Yukio Morii

J. Am. Chem. Soc., **2005**, 127 (10), 3491-3495• DOI: 10.1021/ja0449224 • Publication Date (Web): 19 February 2005

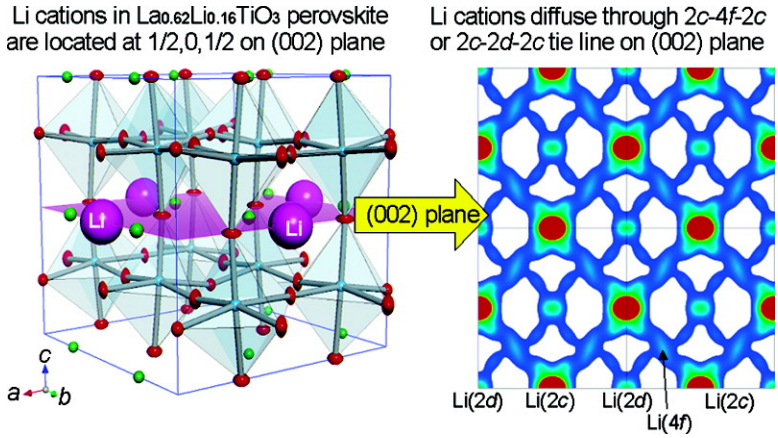

More About This Article

Additional resources and features associated with this article are available within the HTML version:

- Supporting Information
- Links to the 13 articles that cite this article, as of the time of this article download
- Access to high resolution figures
- Links to articles and content related to this article
- Copyright permission to reproduce figures and/or text from this article

View the Full Text HTML

J|A|C|S
ARTICLES
Published on Web 02/19/2005

Crystal Structure and Diffusion Path in the Fast Lithium-Ion Conductor $La_{0.62}Li_{0.16}TiO_3$

Masatomo Yashima,*,† Mitsuru Itoh,‡ Yoshiyuki Inaguma,§ and Yukio Morii||

Contribution from the Department of Materials Science and Engineering, Interdisciplinary Graduate School of Science and Engineering, Tokyo Institute of Technology, Nagatsuta-cho 4259, Midori-ku, Yokohama-shi, Kanagawa, 226-8502, Japan, Materials Structures Laboratory, Tokyo Institute of Technology, Nagatsuta-cho 4259, Midori-ku, Yokohama-shi, Kanagawa, 226-8503, Japan, Department of Chemistry, Faculty of Science, Gakushuin University, 1-5-1 Mejiro, Toshima-ku, Tokyo, 171-8588, Japan, and Japan Atomic Energy Research Institute, Tokai-mura, Naka-gun, Ibaraki, 319-1195, Japan

Received August 23, 2004; E-mail: yashima@materia.titech.ac.jp

Abstract: We report the results of a neutron powder diffraction study of the $La_{0.62}Li_{0.16}TiO_3$ perovskite that determined the diffusion path of lithium cations at room temperature. At 77 K, the Li cations are located at the 2*c* site (Wycoff notation of the *Cmmm* space group) on the (002) La deficient layer, while, at room temperature, they are spread over a wide area and migrate following the 2*c*−4*f*−2*c* or 2*c*−2*d*−2*c* tie line on the (002) layer. The probability density of Li cations has a minimum between the 2*c* and 4*f* or between the 2*c* and 2*d* positions on the diffusion path in contrast to the previous reports where the bottleneck has been thought to be located at the 2*c*, 2*d*, and 4*f* positions. On the basis of the present structural model, the Li-cation conductivity is discussed in terms of a two-dimensional bond-percolation model for Li-cation diffusion. It was found that the vacancy at the La site is essential for the Li-cation conduction.

Introduction

Solid materials with a high lithium-ion conductivity are of vital importance for the development of all-solid-state lithium batteries.[1,2] The discovery of the lithium-doped lanthanum titanate ABO_3 perovskite, (A = $La_{2/3-x}$ and B = Ti) $La_{2/3-x}Li_{3x}TiO_3$, has stimulated wide interest because it is the highest bulk Li-cation conducting solid electrolyte.[2−4] The development of better electrolyte materials requires a better understanding of the mechanism of ionic conduction, and crucial to this is a comprehensive knowledge of the crystal structure.[5] Therefore, a number of researchers have studied the crystal structure of $La_{2/3-x}Li_{3x}TiO_3$ materials.[2,6−13] The crystal structure of the $La_{2/3-x}Li_{3x}TiO_3$ materials has a three-dimensional framework of corner-sharing TiO_6 octahedra and a large number of defects at the A site. Despite numerous structural studies, the exact position of the Li cation is not still clear. Several mechanisms of Li-cation diffusion in $La_{2/3-x}Li_{3x}TiO_3$ compounds have been proposed.[2,6−12,14−17] However, until now, the diffusion path of the lithium cation has not yet been determined. We report the results of a neutron powder diffraction study of the $La_{0.62}Li_{0.16}TiO_3$ perovskite that determined the diffusion path of lithium cations at room temperature.

Experimental Section

The work described here utilizes a $La_{0.62(2)}Li_{0.16(1)}TiO_{3.01(3)}$ sample prepared by solid-state reactions.[9] The sample was furnace-cooled after sintering at 1350 °C. The molar ratio of the cation was determined by inductive coupled plasma spectroscopy. The position and the diffusion path of the Li cation in the sample were studied by neutron diffraction, because there is no interference from the electron-density distribution and the scattering power for Li is relatively large in contrast to X-ray diffractometry. The neutron powder diffraction data were collected at room temperature and at 77 K using the high-resolution angle-dispersive type neutron powder diffractometer (HRPD) installed at the Japan

† Department of Materials Science and Engineering, Tokyo Institute of Technology.
‡ Materials and Structures Laboratory, Tokyo Institute of Technology.
§ Gakushuin University.
|| Japan Atomic Energy Research Institute.

(1) Tarascon, J.-M.; Armand, M. *Nat. Mater.* **2001**, *414*, 359−367.
(2) Stramare, S.; Thangadurai, V.; Weppner, W. *Chem. Mater.* **2003**, *10*, 3947−3990.
(3) Belous, A. G.; Novitskaya, G. N.; Polyanetskaya, S. V.; Gornikov, Y. I. *Izv. Akad. Nauk SSSR, Neorg. Mater.* **1987**, *23*, 470−472.
(4) Inaguma, M.; Chen, Y. L.; Itoh, M.; Nakamura, T.; Uchida, T.; Ikuta, H.; Wakihara, M. *Solid State Commun.* **1993**, *86*, 689−693.
(5) Yashima, M.; Nomura, K.; Kageyama, H.; Miyazaki, Y.; Chitose, H.; Adachi, K. *Chem. Phys. Lett.* **2003**, *380*, 391−396.
(6) Fourquet, J. L.; Duroy, H.; Crosnier-Lopez, M. P. *J. Solid State Chem.* **1996**, *127*, 283−294.
(7) Ruiz, A. I.; Lopez, M. L.; Veiga, M. L.; Pico, C. *Solid State Ionics* **1998**, *112*, 291−297.
(8) Alonson, J. A.; Sanz, J.; Santamaria, J.; Leon, C.; Varez, A.; Fernandez-Diaz, M. T. *Angew. Chem., Int. Ed.* **2000**, *39*, 619−621.
(9) Inaguma, Y.; Katsumata, T.; Itoh, M.; Morii, Y. *J. Solid State Chem.* **2002**, *166*, 67−72.
(10) Sanz, J.; Alonson, J. A.; Varez, A.; Fernandez-Diaz, M. T. *J. Chem. Soc., Dalton. Trans.* **2002**, 1406−1408.
(11) Rivera, A.; Leon, C.; Santamaria, J.; Varez, A.; V'yunov, O.; Belous, A. G.; Alonso, J. A.; Sanz, J. *Chem. Mater.* **2003**, *14*, 5148−5152.
(12) Varez, A.; Inaguma, Y.; Fernandez-Diaz, M. T.; Alonso, J. A.; Sanz, J. *Chem. Mater.* **2003**, *15*, 4637−4641.
(13) Garcia-Martin, S.; Alario-Franoco, M. A.; Ehrenberg, H.; Rodriguez-Carvajal, J.; Amador, U. *J. Am. Chem. Soc.* **2004**, *126*, 3587−3596.
(14) Inaguma, Y.; Yu, J.; Shan, Y.-J.; Itoh, M.; Nakamura, T. *J. Electrochem. Soc.* **1995**, *142*, L8−L11.
(15) Shan, Y. J.; Inaguma, Y.; Itoh, M. *Solid State Ionics* **1995**, *79*, 245−251.
(16) Katsumata, T.; Matsui, Y.; Inaguma, Y.; Itoh, M. *Solid State Ionics* **1996**, *86−88*, 165−169.

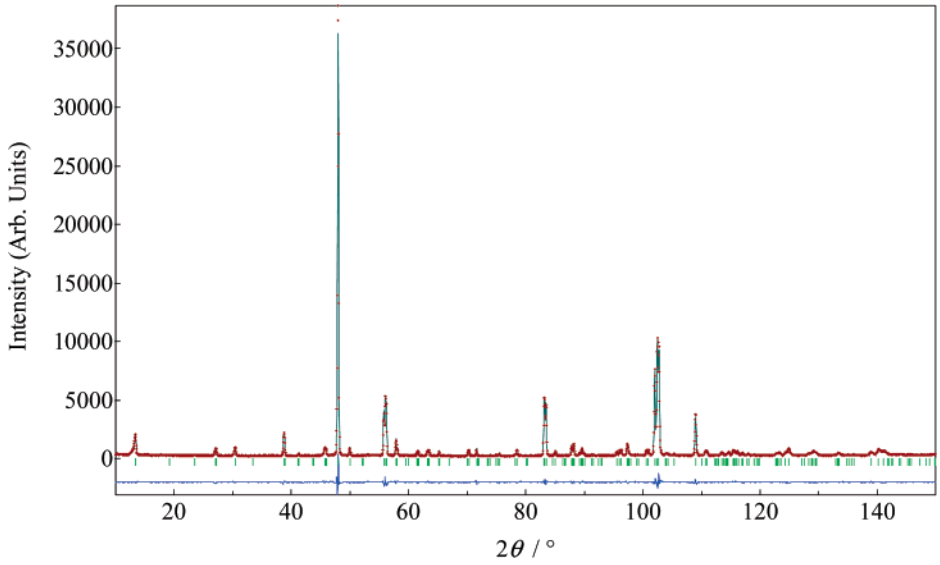

Figure 1. MEM-based whole pattern fitting result for neutron-diffraction data of $La_{0.62}Li_{0.16}TiO_{3.0}$ measured at room temperature. Red crosses (+ symbols) and green line denote observed and calculated intensities, respectively. The short green vertical lines denote the possible Bragg peak positions for the $La_{0.62}Li_{0.16}TiO_{3.0}$. The blue profile denotes the difference between the observed and calculated intensities.

Research Reactor JRR-3M in the Japan Atomic Energy Research Institute (JAERI).[18] The wavelength of the incident neutrons and $\delta(d)/d$ resolution were 1.823 Å and 0.3%, respectively. Powder patterns were obtained in the range from $2\theta = 10°$ to 150°. The diffraction profiles measured at room temperature and 77 K suggested an orthorhombic *Cmmm* structure.[9]

The neutron-diffraction data were iteratively analyzed by a combination of the Rietveld analysis,[19,20] the maximum-entropy method (MEM),[21,22] and the MEM-based pattern fitting (MPF).[23,24] A computer program, RIETAN-2000,[20] was utilized for the Rietveld analysis and MEM-based whole pattern fitting. It is well-known that the MEM can produce a nuclear density distribution map from the neutron diffraction data.[5,23−25] In the MEM analysis, any kind of complicated nuclear density distribution is allowed as long as it satisfies the symmetry requirements. The MEM calculations were performed using the computer program PRIMA,[24] with 128 × 128 × 128 pixels.

Results and Discussion

First, the Rietveld analysis was performed with various structural models in which the positions and occupancies of the Li cations were different from each other. The isotropic and anisotropic harmonic atomic displacement parameters were used for the cations and anions, respectively. Second, the MEM analysis was done using the structural factors obtained by the Rietveld analysis. We consider that the MEM results obtained here are reliable because (1) the number of these factors was 174 for both the data measured at room temperature and 77 K and (2) we used the peak intensity of the 001 reflection at the lowest 2θ position, the reflection that contributes the most information to the analysis. To reduce the bias imposed by the simple structural model, an iterative procedure named the REMEDY cycle[23,24] was employed after the MEM analysis until no significant improvement was obtained.

We have performed the MEM-based whole pattern fitting analysis using the structural factors obtained by the Rietveld analysis with various structural models, to determine both the exact position and diffusion path of the Li cations. The structural models in the literature[9,10,12,13] were found to be inappropriate, because (1) the nuclear density obtained after the REMEDY cycle was inconsistent with these models used in the Rietveld analyses and/or (2) the agreement between the calculated and observed intensities was worse than that in the following new model. The structural model in which the Li cations are located at the 2*c* site (Wycoff notation in the *Cmmm* space group, corresponding fractional coordinate: $^1/_2$, 0, $^1/_2$) gave the lowest *R* factors based on the Bragg intensities, R_I, in the MEM-based whole pattern fitting. The resultant calculated profiles agreed well with the observed ones (Figure 1). The refined crystal parameters are shown in Table 1.

Figure 2 shows the crystal structure of $La_{0.62}Li_{0.16}TiO_3$ at room temperature depicted using the refined crystal parameters. It has a superstructure of $a \approx 2a_p \times b \approx 2a_p \times c \approx 2a_p$ where the subscript p denotes a pseudo ideal cubic perovskite cell. The $La_{0.62}Li_{0.16}TiO_3$ compound has a layered perovskite-type structure consisting of (1) the La-rich (001) La1−O1 layer, (2) the (004) Ti−O layer, and (3) the La-deficient (002) La2−O2 layer. The La-rich La1−O1 and La-deficient La2−O2 layers are alternatively arranged along the *c* axis. The TiO_6 octahedron has anti-phase tilting along the *b* axis. These features are consistent with the structural model in the literature.[9]

The Li cation is located at the Wycoff 2*c* site of the *Cmmm* structure: $^1/_2$, 0.0, $^1/_2$ (Figure 2 and Table 1). The Li position would be valid, because the bond valence sum[26] of the Li site +1.02 calculated from the refined crystal structure is consistent with the valence of the Li cation +1. Furthermore, the MEM nuclear density map supported the Li position (Figures 3a,b and

(17) Katsumata, T.; Inaguma, Y.; Itoh, M.; Kawamura, K. *J. Ceram. Soc. Jpn.* **1999**, *107*, 615−621.
(18) Morii, Y. *J. Crystallogr. Soc. Jpn.* **1992**, *34*, 62−69.
(19) Rietveld, H. M. *J. Appl. Crystallogr.* **1969**, *2*, 65−71.
(20) Izumi, F.; Ikeda, T. *Mater. Sci. Forum* **2000**, *321−324*, 198−203.
(21) Collins, D. M. *Nature* **1982**, *298*, 49−51.
(22) Takata, M.; Umeda, B.; Nishibori, E.; Sakata, M.; Saito, Y.; Ohno, M.; Shinohara, H. *Nature* **1995**, *377*, 46−49.
(23) Izumi, F.; Kumazawa, S.; Ikeda, T.; Hu, W.-Z.; Yamamoto, A.; Oikawa, K. *Mater. Sci. Forum* **2001**, *378−381*, 59−64.
(24) Izumi, F.; Dilanian, R. A. *Recent Res. Dev. Phys.* **2002**, *3*, 699−726.
(25) Sakata, M.; Uno, T.; Takata, M.; Howard, C. H. *J. Appl. Crystallogr.* **1993**, *26*, 159−165.
(26) Brese, N. E.; O'Keeffe, M. *Acta Crystallogr.* **1991**, *B47*, 192−197.

Table 1. Refined Crystal Parameters and Reliability Factors of the $La_{0.62}Li_{0.16}TiO_3$[a]

temperature		room temperature					77 K				
			fractional coordinate of atomic position					fractional coordinate of atomic position			
site		*g*	*x*	*y*	*z*	*U* (Å²)	*g*	*x*	*y*	*z*	*U* (Å²)
La1	4*i*	0.950(3)	0.0	0.2529(7)	0.0	0.0103(5)	0.945(3)	0.0	0.2528(6)	0.0	0.0050(5)
La2	4*j*	0.290(3)[b]	0.0	0.253(3)	1/2	0.016(2)	0.296(3)[b]	0.0	0.252(2)	1/2	0.015 (2)
Ti	8*o*	1.0	0.2478(11)	0.0	0.2597(4)	0.0116(6)	1.0	0.2491(10)	0.0	0.2596(4)	0.0073(6)
Li	2*c*	0.64	1/2	0.0	1/2	0.18(3)	0.64	1/2	0.0	1/2	0.12(2)
O1	4*g*	1.0	0.2737(8)	0.0	0.0	0.019[c]	1.0	0.2735(8)	0.0	0.0	0.016[c]
O2	4*h*	1.0	0.2310(10)	0.0	1/2	0.023[c]	1.0	0.2312(9)	0.0	1/2	0.018[c]
O3	8*m*	1.0	1/4	1/4	0.2356(5)	0.018[c]	1.0	1/4	1/4	0.2351(5)	0.016[c]
O4	4*k*	1.0	0.0	0.0	0.2151(5)	0.012[c]	1.0	0.0	0.0	0.2137(5)	0.008[c]
O5	4*l*	1.0	0.0	1/2	0.2575(6)	0.016[c]	1.0	0.0	1/2	0.2587(5)	0.010[c]
cell parameters		$a = 7.73355(8)$ Å, $b = 7.75422(8)$ Å, $c = 7.78620(7)$ Å					$a = 7.72453(8)$ Å, $b = 7.74690(8)$ Å, $c = 7.77558(8)$ Å				
reliability factors[d]		$R_{wp} = 7.09\%$, $R_p = 5.47\%$, goodness of fit = 1.60, $R_I = 2.93\%$, $R_F = 3.40\%$					$R_{wp} = 7.33\%$, $R_p = 5.54\%$, goodness of fit = 1.69, $R_I = 3.43\%$, $R_F = 3.62\%$				
reliability factors[e]		$R_{wp} = 7.06\%$, $R_p = 5.46\%$, goodness of fit = 1.59, $R_I = 2.84\%$, $R_F = 2.80\%$					$R_{wp} = 7.14\%$, $R_p = 5.50\%$, goodness of fit = 1.64, $R_I = 2.63\%$, R_F=2.65%				

[a] Note: Orthorhombic space group *Cmmm* (No.65) *Z*=8. *g*, occupancy; *U*, atomic displacement parameters. [b] Occupancy for M atom *g*(M) is constrained as follows: *g*(La2) = 1.28 − *g*(La1). [c] Equivalent isotropic atomic displacement parameters calculated by the refined anisotropic values (Å²); U_{13}(O*i*) = U_{23}(O*i*) = 0.0 (*i* = 1, 2, 3, 4, 5); U_{12}(O*j*) = 0.0 (*j* = 1, 2, 4, 5). At room temperature U_{11}(O1) = 0.022(3), U_{22}(O1) = 0.024(2), U_{33}(O1) = 0.0113(15); U_{11}(O2) = 0.026(3), U_{22}(O2) = 0.037(3), U_{33}(O2) = 0.0064(15); U_{11}(O3) = 0.0128(16), U_{22}(O3) = 0.0093(12), U_{33}(O3) = 0.031(2), U_{12}(O3) = −0.002(2); U_{11}(O4) = 0.011(3), U_{22}(O4) = 0.011(3), U_{33}(O4) = 0.014(2); U_{11}(O5) = 0.003(3), U_{22}(O5) = 0.019(4), U_{33}(O5) = 0.024(2), while at 77 K U_{11}(O1) = 0.014(3), U_{22}(O1) = 0.026(2), U_{33}(O1) = 0.0080(15); U_{11}(O2) = 0.016(3), U_{22}(O2) = 0.029(2), U_{33}(O2) = 0.0096(16); U_{11}(O3) = 0.0111(15), U_{22}(O3) = 0.0047(11), U_{33}(O3) = 0.032(2), U_{12}(O3) = −0.006(2); U_{11}(O4) = 0.011(3), U_{22}(O4) = 0.003(3), U_{33}(O4) = 0.011(2); U_{11}(O5) = 0.001(3), U_{22}(O5) = 0.012(3), U_{33}(O5) = 0.016(2). [d] Reliability factors in the Rietveld analysis. [e] Reliability factors in the second and first MEM-based pattern fittings for the data measured at rt and 77 K, respectively.

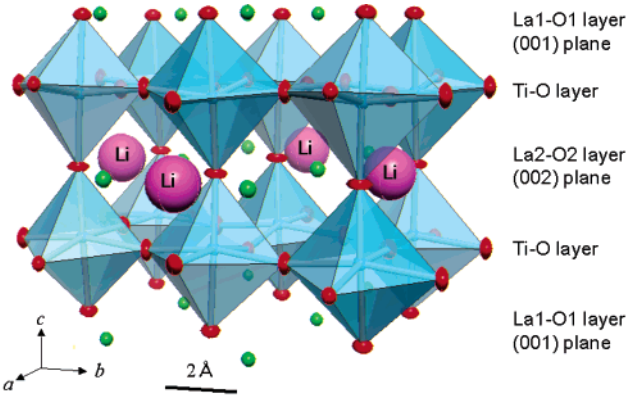

Figure 2. Crystal structure of the layered perovskite-type lanthanum titanate $La_{0.62}Li_{0.16}TiO_{3.0}$ depicted using crystal parameters obtained by the Rietveld analysis of the neutron-diffraction data measured at room temperature. The pink, green, and blue spheres and red ellipsoids denote Li, La, Ti, and oxygen ions, respectively. The blue square is a TiO_6 octahedron.

4a,b). Since the Li cations are not located at the 4*j* A-site proposed in the literature but at the 2*c* site, the chemical formula of the title compound is not $(La_{0.62},Li_{0.16},(Va_{A-site})_{0.22})_{A-site}TiO_3$ but $(La_{0.62},(Va_{A-site})_{0.38})_{A-site}(Li_{0.16},(Va_{2c})_{0.09})_{2c}TiO_3$. Here Va_{A-site} denotes the vacancy at the A-site. $(La_{0.62},Li_{0.16},(Va_{A-site})_{0.22})_{A-site}$ means that the La atom, Li atom, and Va_{A-site} exist at the A-site of the pseudo ABO_3 perovskite-type structure and their occupancies are 0.62, 0.16, and 0.22, respectively. The large atomic displacement parameter of the Li cation indicates the positional disorder and suggests its diffusion. The Li cations are located on the (002) La2−O2 layer (Figure 2), suggesting that the Li cations two-dimensionally diffuse on the La deficient layer. Li cations do not exist on the La1−O1 and Ti−O layers probably because of the higher electrostatic energies. This indicates that the vacancy at the La2 site is a predominant factor for the existence of Li cations on the La2−O2 layer.

To assist in visualizing the disorder and diffusion path, the MEM nuclear density distribution map in the vicinity of the (002) plane is shown in Figures 3 and 4. The nuclear density distribution provided much information on the time and spatially averaged complicated disorder and diffusion path of the Li cations (Figures 3 and 4). Simple models consisting of atom spheres were no longer appropriate to describe the positional distribution of Li cations at room temperature.

At 77 K, most of the Li cations are located near the Wycoff 2*c* site and a very small amount of Li cations exists at the 2*d* position (Figures 3a and 4a). On the contrary, at room temperature, the Li cations exhibit a very large distribution (Figures 3b and 4b), which is consistent with the high Li-cation conductivity at higher temperature.[2−4] There exist anisotropic distributions of Li cations at the 2*c* site in the direction to the nearest neighbor 2*c* position at room temperature and 77 K, suggesting a diffusion path at room temperature. A mild peak exists at the 2*d* site at room temperature and at 77 K. The other mild peak is observed at the 4*f* site at room temperature. It should be noted that the 2*c*, 2*d*, and 4*f* positions of the Li cations are clearly distinguished from the La-deficient La2 site and are located in the packing voids of the La and oxygen atom spheres on the La2−O2 layer (Figure 3c). The Li cations are 4-fold coordinated with oxygen ions, and their bond-valence-sum[26] values are in the range from 0.95 to 1.1, supporting the present Li positions. Most of Li cations are located at the 2*c* position, because the void at this site is larger than those at the 2*d* and 4*f* sites. In fact, the Li(2*c*)−O interatomic distance of 2.08 Å was larger than the others of 1.79−1.94 Å (Figure 3c). The different Li−O distances are ascribed to the tilting of the TiO_6 octahedron, indicating the importance of the tilting for the Li position and diffusion.

The most striking feature is the diffusion path of the Li cations. The path follows the 2*c*−4*f*−2*c* tie lie as shown in Figure 4b and by the pink arrows in Figure 3b. The other possible diffusion path lies on the 2*c*−2*d*−2*c* tie line as shown in Figure 4b and by the pink dashed arrows in Figure 3b. These experimental paths could be consistent with some theoretical

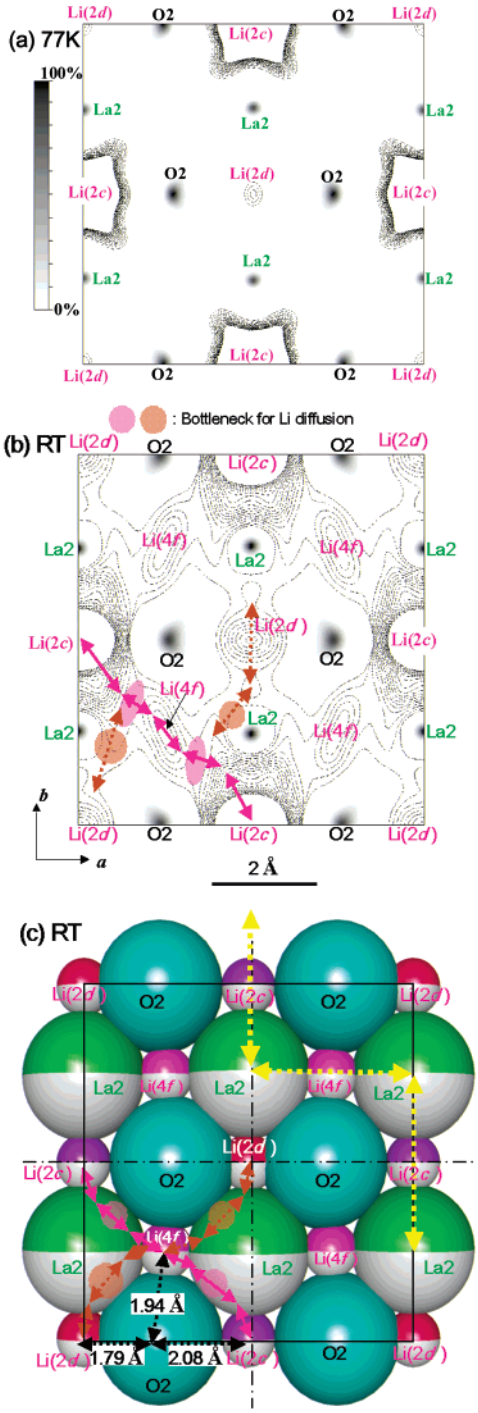

Figure 3. Scattering amplitude distribution in the vicinity of the (002) plane ($0.35 < z < 0.65$) of $La_{0.62}Li_{0.16}TiO_{3.0}$ at (a) 77 K and (b) room temperature. Contour in the range from −1.00 to −0.05 fm/Å^2 (0.05 fm/Å^2 per step). (c) Atomic arrangement on the (002) plane where the ionic radii after Shannon[28] are used to draw the atom spheres. Li atoms are placed at the 2*c*, 2*d*, and 4*f* sites with interatomic distances between the Li and oxygen atoms. The pink arrow indicates a diffusion path. The pink hatched region denotes a possible bottleneck for the Li cation diffusion. The orange dashed arrows are the other possible diffusion paths with a bottleneck indicated by the orange hatched region. The yellow dashed line with arrows is the diffusion path from the literature.

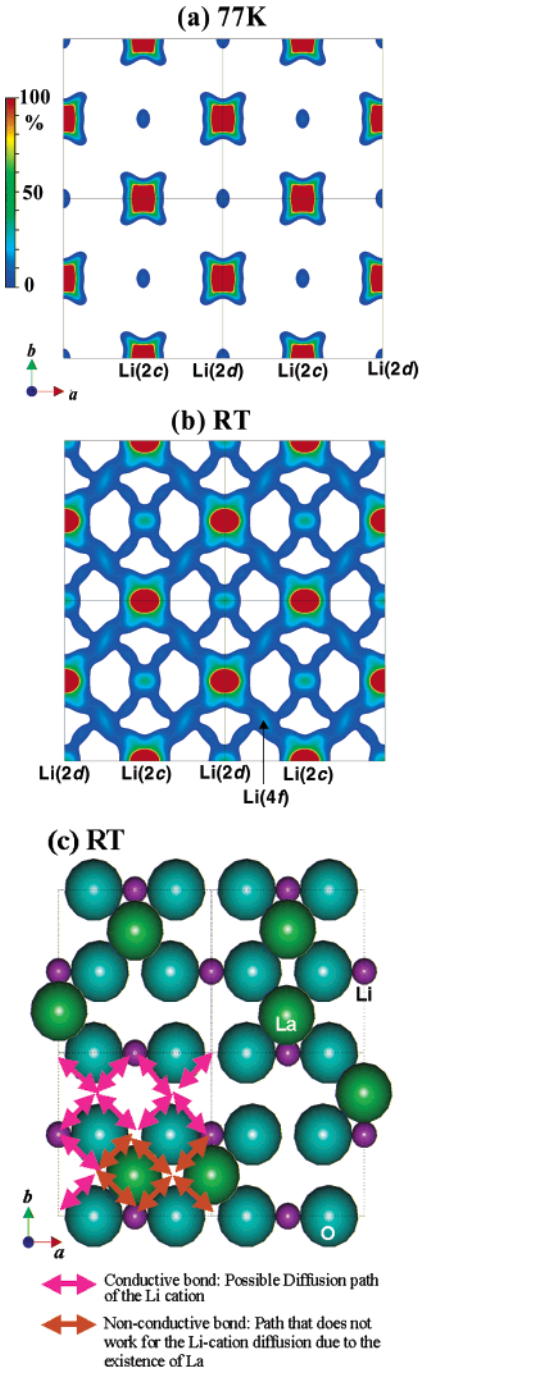

Figure 4. Scattering amplitude distribution on the (002) plane of $La_{0.62}Li_{0.16}TiO_{3.0}$ at (a) 77 K and (b) room temperature where only the distribution for minus scattering amplitude values are drawn to indicate the diffusion paths of the Li cations. The colors red (100%) and blue (0%) correspond to the 0.01% of the maximum scattering amplitude value and 0.004 fm/Å^3, respectively. (c) Atomic arrangement on the (002) plane where the ionic radii after Shannon[28] are used to draw the atom spheres. Li atoms are placed at the 2*c* site. The pink bond with arrows indicates a possible diffusion path of the Li cations, while the orange bond with arrows stands for a diffusion path that does not work for the Li-cation diffusion due to the existence of La ion at the La2 site. In a *Cmmm* unit cell (dot line), 16 bonds exist and one La ion makes four orange bonds.

calculations results.[17,27] However, in many reports,[2,14] the diffusion path of the Li cations has been thought to follow the zigzag line through a vacant La2 site (dashed line in Figure 3c). On the contrary, the MEM nuclear density map clearly indicates that the Li cation directly migrates from the 2*c* to 4*f* site, keeping the Li−O distance constant to some degree. Li cations are unstable at the La2 site because the bond valence

(27) Inaguma, Y.; Matsui, Y.; Yu, J.; Shan, Y.-J.; Nakamura, T.; Itoh, M. *J. Phys. Chem. Solids* **1997**, *38*, 843−852.

sum at the La2 site is estimated to be 2.3, suggesting that the zigzag path through the La2 site is inappropriate.

It should be noted that the probability density of Li cations has a minimum between La2 and O2 atoms on the diffusion path (pink hatched regions in Figure 3b). The position would correspond to the "bottleneck" where the potential energy of a Li cation is the highest on the diffusion path. On the contrary, the bottleneck has been believed to exist at the 2*c*, 2*d*, and 4*f* sites between the La2 and La2 positions in the literature.[2,14]

The "bottleneck" and the diffusion path around the "bottleneck" are located near the La2 position as shown in Figure 3b and c. This strongly suggests that the existence of a La2 ion makes the migration of Li cations difficult near the occupied La2 position due to the coulomb repulsion force between the La2 and Li cations. In fact, the distance between the "bottleneck" and nearest-neighbor La2 cation is 1.4 Å that is much shorter than the sum of the ionic radii[28] of La and Li (1.36 Å + 0.59 Å = 1.95 Å). Therefore, the vacancy at the nearest-neighbor La2 site would be required for the Li-cation diffusion. The conduction channels are linked through the bottleneck with the nearest-neighbor La2 vacancy. This suggests that the Li cations cannot diffuse on the La-rich La1−O1 layer but on the La-deficient La2−O2 one. These results indicate that the existence of a La vacancy is essential for the Li conduction.

In the literature,[29,30] the effect of the carrier concentration and site percolation on the Li-cation conductivity of the lanthanum titanate perovskite has been discussed assuming that all the lithium ions can move independently of each other through the A-site vacancies for conduction: $(La_{2/3-x},Li_{3x},(Va_{A-site})_{1/3-2x})_{A-site}TiO_3$. Here $(La_{2/3-x},Li_{3x},(Va_{A-site})_{1/3-2x})_{A-site}$ means that the La atom, the Li atom, and the vacancy exist at the A-site and their fractions are $2/3 - x$, $3x$, and $1/3 - 2x$, respectively. Since the Li cation does not exist at the A-site (4*j* site in the *Cmmm* structure) but at the 2*c* site, we need to revise the formulation of the effective carrier concentration n_{eff}. In the *Cmmm* $(La_{2/3-x},(Va_{A-site})_{1/3+x})_{A-site}(Li_{3x},(Va_{2c})_{1/4-3x})_{2c}TiO_3$, the n_{eff} is expressed as

$$n_{eff} \propto m(1 - m) = 12x(1 - 12x) \qquad (1)$$

where *m* stands for the ratio of the Li concentration to the sum of the Li and vacancy concentrations at the 2*c* site. The 2*c* site produces a two-dimensional square lattice (Li cations exist at the lattice points in Figure 4c). In a unit cell of the *Cmmm* structure, there exist 16 bonds which could be diffusion paths of the Li cations as shown by the arrows in Figure 4c; however, a La ion makes four nonconductive bonds that do not work as diffusion paths of the Li cation. Thus the conductivity σ is described using the theory of "bond percolation"[31] as

$$\sigma \propto n_{eff}(n' - n_c)^{\mu} = m(1 - m)(n' - n_c)^{1.3} = 12x(1 - 12x)(0.5 - g(\mathrm{La2}))^{1.3} \qquad (2)$$

Here the μ, n', and n_c are the percolation exponent, the concentration of conductive Li−Li bond and the bond-percolation threshold, respectively. Equation 2 clearly indicates that the vacancy at the La2 site and its concentration $1 - g$(La2) are essential for the Li conduction.

The present new structural model and the diffusion path of the Li cations for the $La_{0.62}Li_{0.16}TiO_3$ perovskite would be helpful for developing the mechanism of Li-cation conduction and better Li-cation conductors. It is well-known that the Li-cation conductivity is strongly dependent on the composition of the Li cations $3x$ in the $La_{2/3-x}Li_{3x}TiO_3$ material, temperature, and preparation method such as the cooling rate after sintering. To describe the dependence, further studies are necessary to explore the effect of these factors on the details of the crystal structure and the distribution of Li cations.

Concluding Remarks

We have reported the results of a neutron powder diffraction study of $La_{0.62}Li_{0.16}TiO_3$ perovskite that determines the diffusion path of lithium cations at room temperature. At 77 K, the Li cations are located at the 2*c* site on the (002) La deficient layer, while, at room temperature, they spread over a wide area and migrate following the 2*c*−4*f*−2*c* or 2*c*−2*d*−2*c* tie line. We have demonstrated that the probability density of Li cations has a minimum between the 2*c* and 4*f* or between the 2*c* and 2*d* positions on the diffusion path, in contrast to the previous reports where the bottleneck has been thought to be located at the 2*c*, 2*d*, and 4*f* positions. Since most of the Li cations are not located at the 4*j* A-site but at the 2*c* site, the chemical formula of the title compound is not $(La_{2/3-x},Li_{3x},(Va_{A-site})_{1/3-2x})_{A-site}TiO_3$ but $(La_{2/3-x},(Va_{A-site})_{1/3+x})_{A-site}(Li_{3x},(Va_{2c})_{1/4-3x})_{2c}TiO_3$. The present conclusion would be helpful when discussing the conduction mechanism of Li-ion conductors.

Acknowledgment. We thank Dr. H. Ohno for arranging the neutron-diffraction experiment and Mr. Y. Shimojo and the members of the JRR-3 Operation Division, Department of Research Reactor Operation, JAERI, for their help with the neutron-diffraction experiment. We also thank Mr. M. Mori and Mr. W. Nakamura for the discussions. This research work was partially supported by the Ministry of Education, Science, Sports and Culture, Grant-in-Aid for Scientific Research (B). Figures 2−4 were drawn using the computer program VENUS made by Dr. R. Dilanian and Dr. F. Izumi.

JA0449224

(28) Shannon, R. D. *Acta Crystallogr.* **1976**, *A32*, 751−767.
(29) Kawai, H.; Kuwano, J. *J. Electrochem. Soc.* **1994**, *147*, L78−L79.
(30) Inaguma, Y.; Itoh, M. *Solid State Ionics* **1996**, *86−88*, 257−260.
(31) Stauffer, D.; Aharony, A. *Introduction to Percolation Theory*; Taylor & Haras: London, 1992.